

Impact of transformer saturation from GIC on power system voltage regulation

L. Gérin-Lajoie, S. Guillon, J. Mahseredjian, O. Saad

Abstract - Geomagnetically induced currents (GICs) affect power systems by causing transformer saturation. The primary effects of saturation on the grid, are increased harmonic current injections and var losses. This paper focuses on the second aspect. This paper uses detailed models for developing test cases for GIC simulations. All simulations are performed using an electromagnetic transient (EMT) type tool (EMTP-RV). It is demonstrated that such a tool can be advantageously used to simulate GIC effects in power systems with very accurate models. In addition to three simple test cases for analyzing GIC impact on power system performance, this paper proposes a benchmark case based on the IEEE-39 bus system. Voltage regulation aspects are emphasized.

Keywords: GIC, EMTP-RV, automatic voltage regulator, transformer saturation

I. INTRODUCTION

Geomagnetically induced currents (GICs) have received much attention in the recent years due to their impact on pipelines, telecommunication grids and power transmission grids. GIC is a direct manifestation at ground level of space weather [1]. GIC can cause problems, such as increased corrosion of pipelines [2][3] and damage to high-voltage power transformers. In electrical systems, the GIC can be represented by a quasi-direct current (dc). When GICs flow through transformer windings, they create a flux offset that can drive the core into deep saturation for one-half of the power cycle. The primary effects of half-cycle saturation on the grid are increased harmonic current injection and var losses. The increases in reactive loading are due to the increase in the fundamental component of the exciting current, which can lead to voltage depression, transmission line disconnection and system voltage collapse [5][4]. Power utilities must investigate the GIC risk and develop mitigation strategies.

Recent studies with PSS/E for the 1989 Hydro-Quebec blackout, indicate that additional reactive power loading combined with onload tap changer action in the load area, could have resulted in voltage collapse [16].

Most investigations concern the protection of power transformers [6], the misoperation of protective relays [7] and impact on system stability [8]. Most studies are traditionally

conducted using transient stability type programs. The work presented in this paper is based on the more accurate electromagnetic transient (EMT) analysis approach with EMTP-RV.

This paper presents a set of simulation cases for illustrating the impact of GIC on voltage regulation in the presence of transformer saturation.

II. METHODOLOGY

This paper presents four cases to validate and illustrate the impact of GIC on transformer saturation as well as network voltage regulation. The complexity of the cases is increased in order to assess the importance of using EMT type tools to cover the wideband phenomenon related to GIC. The network transmission lines are represented with frequency dependent models valid from dc up to fourth and sixth harmonic range. The GIC is modeled as a dc voltage source injected in the neutral of transformers or in series with transmission lines. The dc voltage source saturates the transformer. The transformer saturation curve is calibrated with field test measurements to accurately simulate the GIC saturation effect. The synchronous machines are modeled with their saturation curves and all necessary details for accurately replicating transient performance. The automatic voltage regulation (AVR) controls are also included. This is important when analyzing the voltage regulation of the power system.

The proposed methodology is first applied on a simple network with an ideal Thevenin source, three transformers, one line and dc voltage injection in the ground reference. This case is used as a benchmark to establish the best modeling approach for dc injection and transformer grounding strategy. A set of GIC power system indicators (GPSI) are defined using the dc measurements of current and flux in the transformer. Another important indicator used in the voltage regulation assessment is the difference in Mvars (ΔQ) between the primary and secondary windings of transformers.

The second test case represents a four substation network from north to south. This case demonstrates that the GIC impact is only present on the two extremities. In the middle substation the GIC dc impact is cancelled.

The third case extends the second case to a 4 by 4 substation network to determine the maximum and minimum indicators based on the geomagnetic storm orientation (GSO).

Finally, a more complex case representing the IEEE-39 bus system is simulated to study the effect of cumulative ΔQ on the network's voltage regulation and to demonstrate the possibility of voltage collapse.

Luc Gérin-Lajoie, TransÉnergie, Hydro-Québec.
(email of corresponding author : gerin-lajoie.luc@hydro.qc.ca).

Sébastien Guillon, TransÉnergie, Hydro-Québec.

Omar Saad is with IREQ, Hydro-Québec.

Jean Mahseredjian is with École Polytechnique, Montréal, Québec.

III. TRANSFORMER MODEL

The transformer nonlinear saturation curve is calibrated with field test measurements [9] using a single phase transformer (765/120 kV – 300MVA). The relation between magnetic flux and current was recalculated in pu-pu and can be used for power transformers with different ratings. In this study all transformers have the same saturation characteristic based on the single phase transformer. The topology of the magnetic circuit may introduce higher reluctance. This aspect is not covered in this study. Other transformer types are presented in [4] and can be eventually analyzed using the network topologies presented in this paper.

IV. CASE-1

To assess the best simulation strategy, Case-1 was simulated using 4 different options. Figure 1 represents the circuit used in the first variant with a single line connecting the two substations. The GIC dc voltage is injected between the grounding points of the substations. To capture the wideband nature of GIC, the 250 km transmission line is modeled using a frequency dependent model covering the frequency range from dc to 1kHz. The grounding impedances were 0.2Ω for T1, 0.1Ω for T2 and T3.

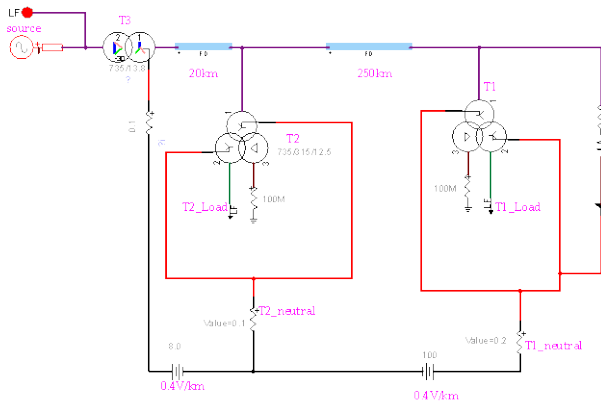


Figure 1 Case-1, dc source in grid grounding and solid load grounding

Another variation of Case-1 is shown in Figure 2, where the GIC dc voltage is injected directly into the transmission line. One important aspect is to study the best grounding strategy of the load: connecting directly to perfect ground or via the grid resistance.

One may expect that the four options – dc in the line versus dc in grid grounding – loads on grid grounding versus perfect ground – should give the same results. But this is not the case in reality. When the loads are directly connected to ground, the choice of the location of the dc source gives different results. Figure 3 shows the saturation current of transformer T1. An induced dc voltage value of $0.5V/km$ for the 250 km line is used in this test.

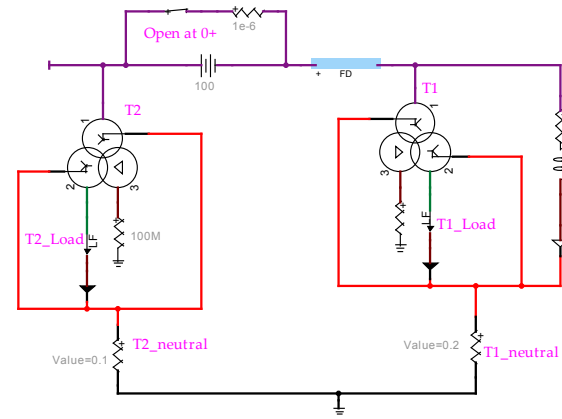


Figure 2 Case-1, dc source in series with the line and load grounded on substation grid

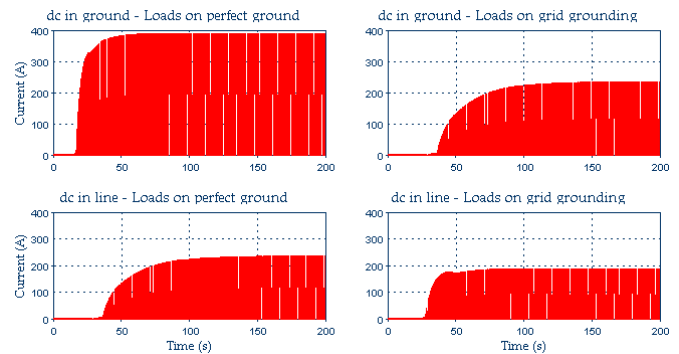


Figure 3 Case-1, saturation of T1, one phase, loads on perfect ground (left) and loads on grid grounding (right), dc source in grid grounding (up) and in the line (down).

Load grounding connections may vary. Figure 4 shows appropriate load grounding techniques. The presence or the absence of grounding bank (zig-zag) at 25kV has no impact on GIC circulation. Another approach is to use ungrounded loads. This approach will be used for all the rest of simulations in this paper. With ungrounded loads, the results shown in Figure 5 indicate that the GIC results do not depend on the dc source location.

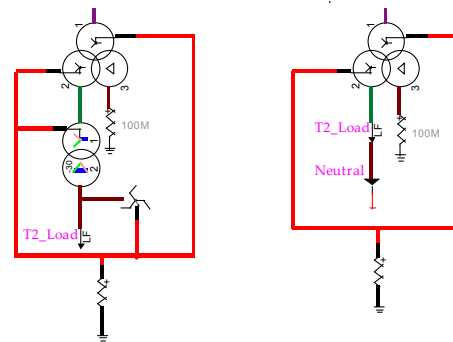


Figure 4 Two valid load grounding methods

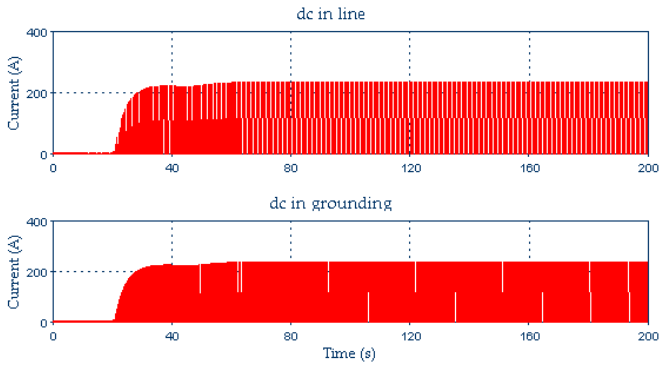


Figure 5 Case-1, saturation of T1, one phase, loads ungrounded, dc source in the line (up) and in grid grounding (down).

The dc impedance circuits of transmission and distribution transformers are not connected together due to transformer delta connections. This explains why the loads have to be ungrounded when simulated without Yd transformers.

Next the effect of the selected line model is studied in order to assess the best modeling approach. To get the correct line impedance for GIC studies, it is important to use a valid frequency-dependent line (FD-line) model in the range of 0-300Hz. To accelerate the simulation, the FD-line model can be replaced by a PI-line. The GIC dc currents are considered as zero sequence. The ratio of line zero-sequence to positive-sequence resistance (R_0/R_1) is typically equal 5 to 30 at fundamental frequency. At 0Hz $R_0=R_1$ and it is necessary to adjust the PI-line models accordingly.

Figure 6 shows the results with both line models. The magnetization current (I_m) of the PI-line is slightly different from the FD-line version, but can be acceptable considering all other unknown GIC parameters. Figure 6 shows that the dc flux continues to increase up to 30s (steady-state). Meanwhile the nonlinear magnetization current increases up to few hundred amperes. The FD-line dc impedance (set at 0.001 Hz) seems to have no effect on the magnetization current. The grounding current amplitude includes only multiples of 3rd harmonic with a predominant 6th harmonic.

Although the usage of PI-lines can be justified for improving computational speed, better accuracy and generality is achieved with wideband models, such as FD-line.

V. GIC POWER SYSTEM INDICATORS

Figure 7 shows GIC power system indicators (GPSI) used in the study of Case-1. The magnetization current includes mainly even harmonics. Therefore 2nd and 4th harmonic current and voltage meters are used. The dc flux is also monitored as well as the 60Hz magnetization branch current (I_m).

The reactive power difference (ΔQ) between the high and low voltage sides of the transformer is also measured in Figure 7. This parameter indicates the supplementary vars the saturated transformer will consume due to GIC. In Figure 7 the transformer T1 (900MVA) requires supplementary 33Mvars.

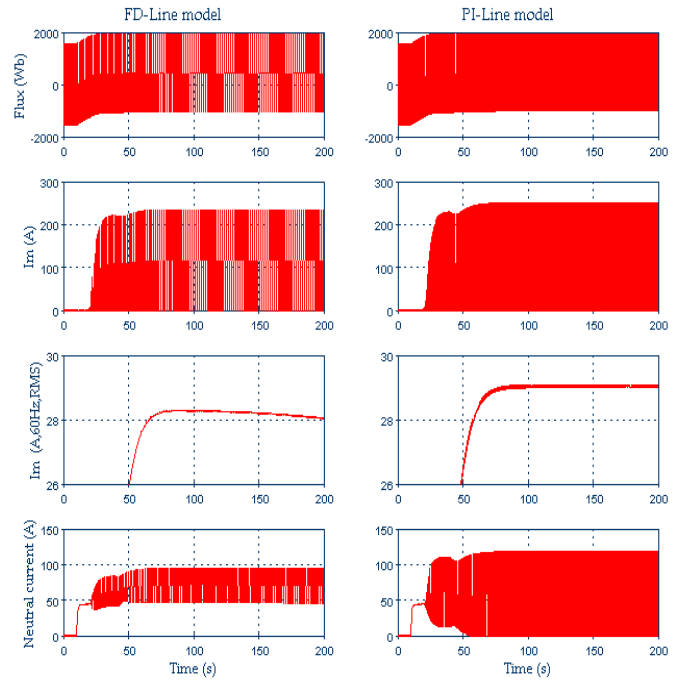


Figure 6 Case-1, FD-line versus PI-line models, transformer T1, I_m is magnetization current

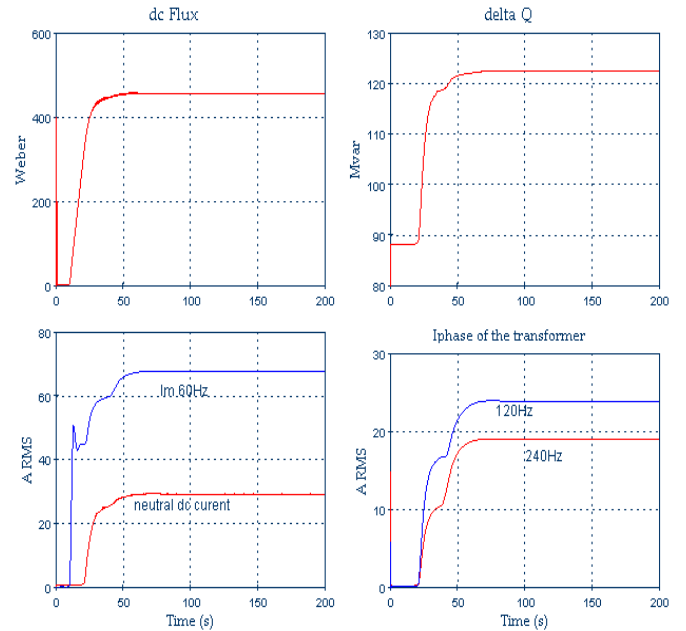


Figure 7 GPSI for GIC detection, Case-1, transformer T1

The transformer leakage resistance and the quality of the substation grounding affect the circulation of current in the transformer neutral. The tables below illustrate the sensitivity to these parameters for Mvar absorption.

TABLE 1
EFFECT OF X/R TRANSFORMER RATIO ON MVAR ABSORPTION

| X/R | T1 | T2 | T3 | Total |
|-----|----|----|------|-------|
| 25 | 12 | 1 | 15 | 28 |
| 50 | 20 | 1 | 19 | 40 |
| 75 | 24 | 2 | 20 | 46 |
| 100 | 27 | 3 | 22 | 52 |
| 150 | 27 | 3 | 21.3 | 51.3 |
| 200 | 32 | 3 | 22 | 57 |

TABLE 2
EFFECT OF NEUTRAL (GROUNDING) RESISTANCE
ON MVAR ABSORTION, X/R=50

| R _{neutral} | T1 | T2 | T3 | Total |
|----------------------|------|-----|------|-------|
| 0 | 22 | 0.3 | 22.7 | 45 |
| 0.05 | 21 | 0.8 | 22 | 43.8 |
| 0.20 | 18.6 | 2 | 16.5 | 37.1 |
| 0.50 | 15.3 | 4.3 | 10.8 | 30.4 |
| 2 | 8 | 3.4 | 4.2 | 15.6 |

The saturated steady-state depends on the amplitude of the dc voltage applied between the ground and the nonlinear inductance branch of the transformer. It also depends on transformer parameters and transformer electrical position in the network. The steady-state dc flux for transformers T1 to T3 is presented in Figure 8.

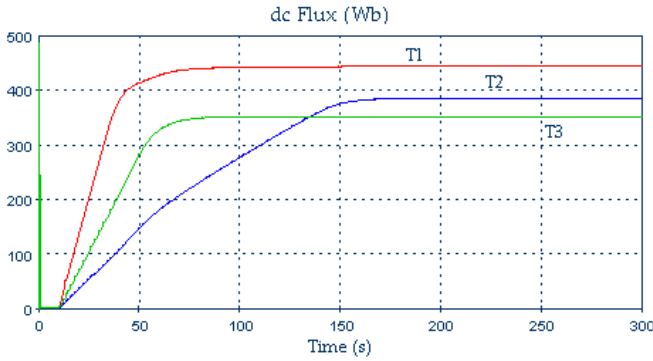


Figure 8 DC flux steady state establishment for T1, T2 and T3

VI. CASE-2 – A FOUR SUBSTATION NETWORK

The GIC impact on transformers depends on network topology. This is further demonstrated in this section using the Case-2 network shown in Figure 9. In this network four equally spaced substations are placed in series. The simulation of this case shows that only the transformers at the extreme ends will saturate. All three-winding transformers are identical and of 1000MVA. The generator transformer is of 3000MVA. The transformers T2 and T3 do not observe dc currents in there neutrals, since each dc circulation loop is in opposite direction and the dc effect is cancelled out as shown in Figure 10.

VII. CASE-3 – 4 BY 4 SUBSTATION NETWORK

The previous case is extended to a 4x4 (16-substations) network oriented north-south and east-west. All lines are identical 250km sections. This case will be used to demonstrate the impact of the Geomagnetic Storm Orientation (GSO) on the saturation amplitude of sixteen transformers. The induced dc voltage is calculated using

$$V_{dc} = V'_{dc} \ell \cos \theta \quad (1)$$

where V_{dc} is the dc source voltage, V'_{dc} is the induced voltage per unit length, ℓ is the line length and θ is the difference between the line orientation (0° or 90°) and the GSO. Three conditions were analyzed: GSO equal to 0° , 45° and 90° . The objective is to determine the impact of GSO on the ΔQ for all transformers. As expected, with GSO= 0° , the

results of Figure 11 correspond to those shown in Figure 10 and no dc current circulates on east-west lines.

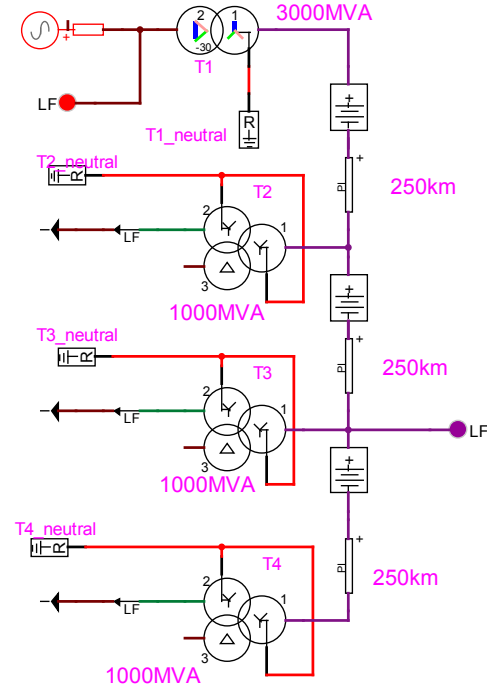


Figure 9 Transformers equally geographically placed in a network

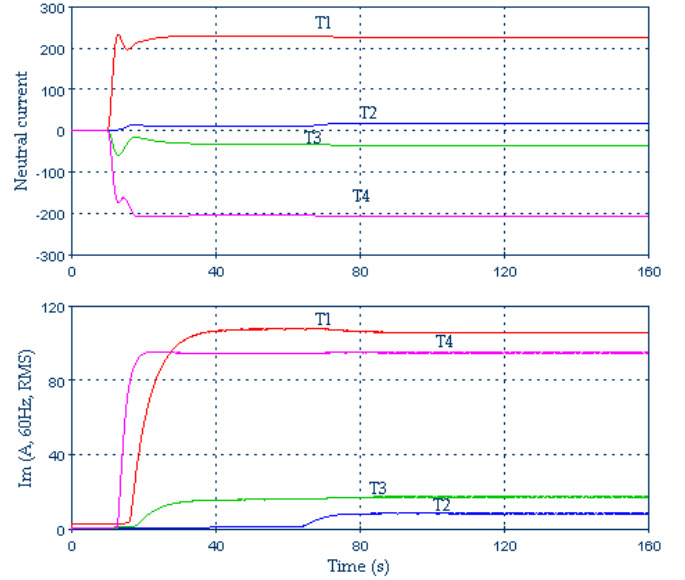


Figure 10 Neutral and magnetization branch currents of transformers in Figure 9

A GSO of 45° causes dc currents in all lines but not necessary in all transformer neutrals. The network topology impacts on the saturation level of transformers.

Table 1 presents transformer total Mvar consumption for three GSOs and $V'_{dc} = 1V/km$ for all lines. This table indicates that the network has a minimum and a maximum total Mvar increase as a function of the GSO.

In normal conditions and depending on the value of the GSO, the total Mvar consumption can double.

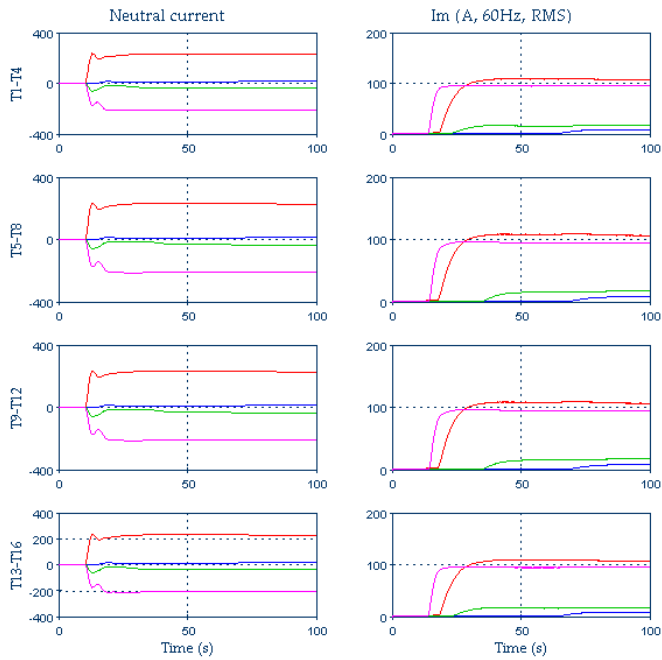


Figure 11 Neutral and magnetization currents, 16 transformers, GSO of 0°

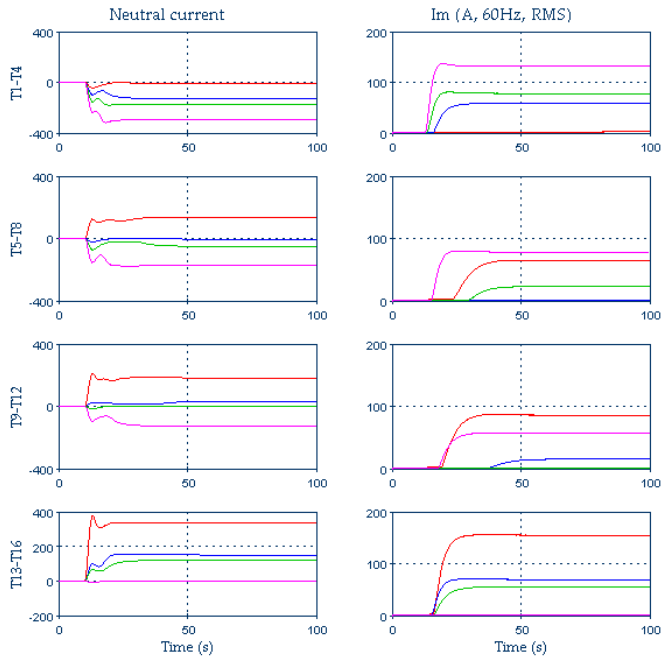


Figure 12 Neutral and magnetization currents, 16 transformers, GSO of 45°

VIII. IEEE-39 BUS CASE

The IEEE-39 bus benchmark [11] is modified for this EMTP GIC study. This system has 10 generators/transformers and 20 loads/transformers. The transformer nominal rated powers were calculated from the initial 100MVA based data. The line lengths were also deduced from typical positive sequence impedances of a 500kV line [12]. PI-Line models have been used to reduce computational timings. Line orientations, i.e. north-south and east-west, are arbitrarily set as indicated in Table 4. All loads are ungrounded and given the exponential load model. All transformers have a Y_d configuration with a total rated power of 17200MVA and all

transformers are grounded with a 0.2Ω resistance.

The generator models include AVRs and saturation data.

TABLE 3
CASE3 – TRANSFORMER REACTIVE POWER (MVAR)
CONSUMPTION INCREASE

| GSO | T1-T4 | T5-T8 | T9-T12 | T13-T16 | $\Sigma(\Delta Q)$ |
|--------------|------------|------------|------------|------------|--------------------|
| 0° | 125 | 125 | 125 | 125 | 500 |
| | 15 | 15 | 15 | 15 | 60 |
| | 23 | 27 | 27 | 23 | 100 |
| | 113 | 116 | 116 | 97 | 442 |
| Total | 276 | 283 | 283 | 260 | 1102 |
| 45° | 0 | 60 | 100 | 170 | 330 |
| | 46 | 15 | 0 | 28 | 89 |
| | 15 | 20 | 0 | 0 | 35 |
| | 100 | 80 | 0 | 0 | 180 |
| Total | 161 | 175 | 100 | 198 | 634 |
| 90° | 132 | 6 | 6 | 133 | 277 |
| | 123 | 32 | 32 | 123 | 310 |
| | 133 | 35 | 35 | 123 | 326 |
| | 133 | 31 | 30 | 134 | 328 |
| Total | 521 | 104 | 103 | 513 | 1241 |

TABLE 4
IEEE-39 BUS NETWORK
ARBITRARY NORTH-SOUTH (NS) LINE ORIENTATION

| BUS | | Length (km) | NS (deg) | BUS | | Length (km) | NS (deg) |
|------|----|-------------|----------|------|----|-------------|----------|
| From | To | | | From | To | | |
| 1 | 2 | 275 | 0 | 13 | 14 | 68 | 34 |
| 1 | 39 | 168 | 2 | 14 | 15 | 145 | 36 |
| 2 | 3 | 101 | 4 | 15 | 16 | 63 | 38 |
| 2 | 25 | 58 | 6 | 16 | 17 | 60 | 40 |
| 3 | 4 | 143 | 8 | 16 | 19 | 131 | 42 |
| 3 | 18 | 89 | 10 | 16 | 21 | 90 | 44 |
| 4 | 5 | 86 | 12 | 16 | 24 | 40 | 48 |
| 4 | 14 | 86 | 14 | 17 | 18 | 55 | 50 |
| 5 | 6 | 17 | 16 | 17 | 27 | 116 | 52 |
| 5 | 8 | 75 | 18 | 21 | 22 | 94 | 54 |
| 6 | 7 | 62 | 20 | 22 | 23 | 64 | 56 |
| 6 | 11 | 55 | 22 | 23 | 24 | 235 | 58 |
| 7 | 8 | 31 | 24 | 25 | 26 | 216 | 60 |
| 8 | 9 | 243 | 26 | 26 | 27 | 99 | 62 |
| 9 | 39 | 168 | 28 | 26 | 28 | 318 | 64 |
| 10 | 11 | 29 | 30 | 26 | 29 | 419 | 10 |
| 10 | 13 | 29 | 32 | 28 | 29 | 101 | 10 |

The total Mvar consumption sensitivity was analyzed with three parameters: GSO, the amplitude of applied dc voltage along the lines, and with and without automatic voltage regulator (AVR) for all generators. Table 5 presents results for total Mvar without AVR. The first line presents the Mvar consumption in normal operation. The ratios are calculated using the Mvar increase over the normal operation values. As indicate on this table, the worst case occurs when the GSO is 45° for both induced voltage intensities. A storm with 5V/km will increase the consumption by 66%.

TABLE 5
TOTAL MVAR CONSUMPTION WITHOUT AVRS
XFO MEANS TRANSFORMER

| GIC voltage (V/km) | GSO (deg) | Load xfo $\Sigma(\Delta Q)$ | Gen xfo $\Sigma(\Delta Q)$ | Load xfo ratio | Gen xfo ratio |
|--------------------|-----------|-----------------------------|----------------------------|----------------|---------------|
| 0 | --- | 940 | 1019 | 100% | 100% |
| 2 | 0 | 1218 | 1330 | 130% | 131% |
| 2 | 22 | 1257 | 1383 | 134% | 136% |
| 2 | 45 | 1275 | 1382 | 136% | 136% |
| 2 | 67 | 1241 | 1330 | 132% | 131% |
| 2 | 90 | 1165 | 1224 | 124% | 120% |
| 5 | 45 | 1565 | 1847 | 166% | 166% |

Table 6 shows that the transformer var consumption impact during the storm is not cancelled by the presence of AVRS. Even if the generators compensate for the var consumptions of their transformers, the load transformers still consume extra vars.

TABLE 6
TOTAL MVAR CONSUMPTION WITH AVR

| GIC voltage (V/km) | GSO (deg) | Load xfo $\Sigma(\Delta Q)$ | Gen xfo $\Sigma(\Delta Q)$ | Gen $\Sigma(Q)$ | Load xfo ratio | Gen xfo ratio |
|--------------------|-----------|-----------------------------|----------------------------|-----------------|----------------|---------------|
| 0 | --- | 940 | 1019 | 1844 | 100% | 100% |
| 2 | 45 | 1241 | 1400 | 2700 | 132% | 137% |
| 5 | 45 | 1780 | 2092 | 3982 | 189% | 205% |

The load voltages listed in Table 7 are for a GIC level of 5V/km. Voltage drops by more than 1.5 to 2.0% cause the tap changers to operate.

TABLE 7
LOAD VOLTAGES (KV), BEFORE AND DURING THE STORM, 5V/KM

| Load id | Load voltage no GIC | Load voltage during GIC | Ratio |
|---------|---------------------|-------------------------|-------|
| 3 | 25.1 | 23.5 | 93% |
| 4 | 24.0 | 22.2 | 92% |
| 7 | 23.4 | 20.5 | 87% |
| 8 | 23.9 | 20.4 | 86% |
| 12a | 24.3 | 22.2 | 91% |
| 12b | 24.3 | 22.2 | 91% |
| 15 | 23.0 | 21.1 | 91% |
| 16 | 24.7 | 22.2 | 90% |
| 18 | 24.6 | 22.4 | 91% |
| 19 | 23.4 | 22.6 | 97% |
| 21 | 22.0 | 19.5 | 89% |
| 23 | 23.6 | 22.1 | 94% |
| 24 | 24.8 | 21.3 | 86% |
| 25 | 23.9 | 22.6 | 94% |
| 26 | 23.6 | 21.6 | 91% |
| 27 | 22.6 | 20.3 | 90% |
| 28 | 23.8 | 21.6 | 91% |
| 29 | 23.8 | 21.9 | 92% |
| 39 | 22.8 | 22.1 | 97% |

Table 8 indicates that the relation between the neutral dc current and var losses caused by saturation is not linear. This ratio varies between 0.32 and 0.50 for the studied network. It is observed that each transformer sees different network Thevenin impedance according to its location.

IX. VOLTAGE COLLAPSE

When the operation point of a power system is close to voltage collapse, the saturation of transformers can easily drive the network into an actual voltage collapse. A voltage collapse depends on many factors; among those are the initial operation point (on the PV curve) and a loss of var control equipment. Typical var control devices are SVC, synchronous compensator and capacitor bank. The omission to remove shunt inductance by the operator is also a contributing factor. To be able to simulate voltage collapse conditions very accurately, it is required to perform unusually long simulations with EMT-type programs. In addition, it is necessary to include various models, such as: transformer tap changer, over excitation limiter (OEL) in the AVR and more accurate (exponential) load models. It has been observed that voltage collapse can occur even with simplified (constant impedance) load models. Worst case summer load settings are used in the proposed IEEE-39 benchmark with $N_p=1.0$ and $N_q=1.8$. These models [13][14][15] were available from previous EMT-P-RV studies and directly used in this paper. The tap changer had 17 positions, with a voltage step of 2%, and a temporization of 10s. The OEL parameters used here correspond to the case of thermal unit. Figure 13 shows the tap changer and OEL operations due to GIC conditions. Power plants 2 (blue) and 3 (green) are the first to collapse.

TABLE 8
RATIO BETWEEN NEUTRAL CURRENT AND MVAR CONSUMPTION, 2V/KM

| Xfo | | Neutral current (A _{dc}) | ΔQ (MVAR) | $\Delta Q/\text{Ineutral}$ |
|--------------|--------|------------------------------------|-------------------|----------------------------|
| Rating (MVA) | Number | | | |
| 200 | 26 | 23.4 | 10.70 | 0.46 |
| 300 | 18 | 26.2 | 11.24 | 0.43 |
| 340 | 12a | 26.6 | 10.10 | 0.38 |
| 340 | 12b | -36.5 | 13.57 | -0.37 |
| 400 | 7 | -75.5 | 30.68 | -0.41 |
| 400 | 21 | -80.9 | 37.84 | -0.47 |
| 400 | 24 | 127.8 | 53.28 | 0.42 |
| 400 | 25 | 7.2 | 2.34 | 0.32 |
| 400 | 27 | 39.8 | 19.13 | 0.48 |
| 400 | 28 | 44.1 | 18.80 | 0.43 |
| 400 | 29 | 63.1 | 27.38 | 0.43 |
| 500 | 3 | -10.5 | 4.82 | -0.46 |
| 500 | 15 | 35.5 | 17.82 | 0.50 |
| 500 | 16 | 81.8 | 35.86 | 0.44 |
| 700 | 4 | 28.2 | 13.08 | 0.46 |
| 700 | 8 | -192.9 | 80.76 | -0.42 |
| 800 | 20 | -50.5 | 0.19 | 0.00 |
| 800 | 23 | -59.1 | 24.13 | -0.41 |
| 1500 | 39 | -7.6 | 0.32 | -0.04 |

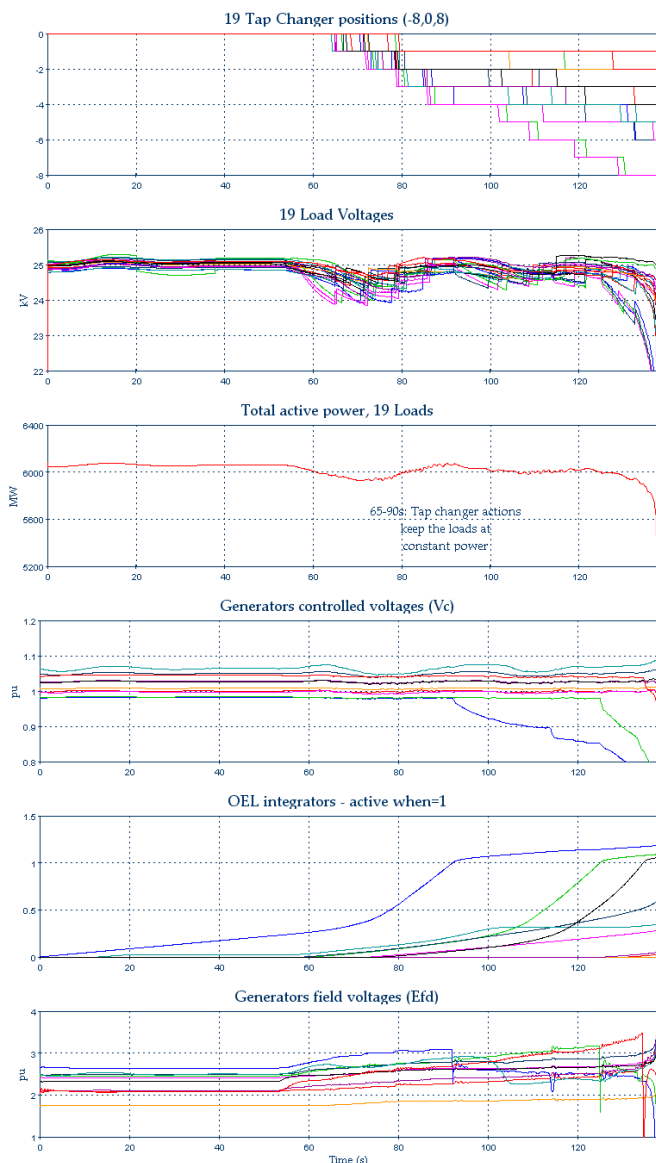


Figure 13 Voltage collapse during a geomagnetic storm, 2V/km

A test case for GIC was proposed in [10]. This paper is proposing to include the modified IEEE-39 bus system as a second test case for GIC studies including detailed voltage collapse simulations.

X. CONCLUSIONS

This paper presented four study cases in order to simulate the impact of GIC on power systems. Case-1 demonstrated that power system components must be modeled accurately using wideband models. The loads were represented with an ungrounded neutral or in series with their Yd transformers to obtain the correct dc solution in the transformer neutrals.

Case-2 studied the impact of substation geographic location. Case-3 demonstrated that for a given power system, the geomagnetic storm orientation (GSO) has an important impact on the injected dc currents and resulting steady-state condition.

Case-4 contributes a modified version of the IEEE-39 bus system with arbitrary transmission line orientations. It is

noticed that with induced dc voltages of 2 and 5V/km, the reactive power consumptions of transformers increase by 36 and 66% respectively. Even if the AVRs are able to control the machine terminal voltages, it is not possible to avoid voltage collapse caused by the saturation of load transformers. It is also observed that the relation between neutral dc current and var losses caused by saturation is not linear.

Finally the present paper demonstrates that EMT-type simulations can be advantageously used to study GIC impact on power systems with accurate/detailed models and for very long simulation intervals.

XI. ACKNOWLEDGEMENT

The authors acknowledge the contribution of B. Khodabakhchian for his help on this study.

XII. REFERENCES

- [1] NERC, "2012 Special Reliability Assessment Interim Report: Effects of Geomagnetic Disturbances on the Bulk Power System," February 2012.
- [2] D.H. Boteler, "Distributed source transmission line theory for electromagnetic induction studies". In Supplement of the Proceedings of the 12th International Zurich Symposium and Technical Exhibition on Electromagnetic Compatibility, pp. 401–408, 1997.
- [3] A. Pulkkinen, R. Pirjola, D. Boteler, A. Viljanen, I. Yegorov, "Modelling of space weather effects on pipelines", Journal of Applied Geophysics, 48, 233-256, 2001.
- [4] L. Bolduc, "GIC observations and studies in the Hydro-Québec power system", J. Atmos. Sol. Terr. Phys., 64(16), 1793–1802, 2002.
- [5] GMDTF Interim report "Effects of geomagnetic Disturbances on the Bulk Power System", NERC, February 2012.
- [6] V. Gurevich, "Protection of Power Transformers Against Geomagnetically Induced Currents", DOI: 10.2298/SJEE1103333G
- [7] "Solar Magnetic Disturbances/Geomagnetically Induced Current and Protective Relaying". Palo Alto, CA: Elect. Power Res. Inst., Aug.1993, EPRI TR-102621.
- [8] J. G. Kappenman, L. L. Grigsby, Ed., "Geomagnetic disturbances and impacts upon power system operation," in Electrical Power Engineering Handbook, 2nd ed. Boca Raton, FL: CRC/IEEE, 2007, ch.16, pp. 16–1–16-22.
- [9] C. Morin, B. Khodabakhchian, "765 kV Power Transformer Losses Upon Energizations: A Comparison Between Field Test Measurements And EMTP-RV Simulations", IPST, Vancouver, July 2013.
- [10] R. Horton, D. Boteler et al. "A test Case for the Calculations of Geomagnetic Induced Currents. IEEE Transaction on Power delivery, Oct. 2012.
- [11] M. A. Pai, "Energy Function Analysis for Power System Stability", Kluwer Academic, 1989
- [12] P.M. Anderson, R.G. Farmer, "Series compensation of Power System", 1996, page 503
- [13] O. Saad, B. Khodabakhchian, "Operation of Tap changer During a Voltage Dip" EMTP-RV/Examples/tap changer", September 2005.
- [14] L. Gérin-Lajoie, "Exponential load model in EMTP", www.emtp.com, Exchange Platform, March 2013.
- [15] L. Gérin-Lajoie, "Extra control of machines - IEEE AVR", www.emtp.com, Exchange Platform, March 2013.
- [16] S. Renaud, "Orage géomagnétique – Panne du 13 mars 1989 et le réseau 2012". Planification et Stratégies du réseau. Rapport interne Hydro-Québec. Novembre 2012.